# Theory of impurity-concentration dependence of freezing temperatures of metallic spin glasses

Mark R. A. Shegelski* and D. J. W. Geldart

*Department of Physics, Dalhousie University, Halifax, Nova Scotia, Canada B3H 3J5*
(Received 27 December 1991)

We present a theory of the freezing temperature $T_g$ of metallic spin glasses. Length scales associated with intrinsic $sd$ scattering and finite temperature play essential roles. We describe an approach in which $T_g$ is calculated directly in terms of the strength and range of the effective spin-spin pair interactions. The theory leads to a clear physical picture of the dependence of $T_g$ on the concentration and type of impurities in the spin glass, and provides a comprehensive account of a wide range of experimental data.

## I. INTRODUCTION

Spin glasses are complex magnetic systems having inherent structural disorder. Localized magnetic moments experience "frustrated interactions" which lead to a freezing transition to a glassy state at a low temperature $T_g$. Dilute alloys of $3d$ transition-metal (TM) impurities in a noble-metal (NM) host (e.g., Ag-Mn) are canonical examples of spin glasses. Since the original description of freezing in spin glasses in 1959 by Blandin and Friedel,[1] many problems have been studied.[2] Despite intense efforts by numerous researchers, many questions remain unresolved.

In this paper, we focus on the following problem. If the fundamental structure of a spin glass is changed, by adding a small concentration of impurities for example, the freezing temperature $T_g$ will also change. What are the physical processes which determine the changes in $T_g$? We will focus on the canonical NM-TM spin glasses, in which the dominant mechanism driving the freezing transition is the indirect exchange interaction $J_{eff}$ between $3d$ magnetic moments. In its simplest form (two moments in an otherwise pure metal at zero temperature), the exchange interaction for spin separation $R \gg k_F^{-1}$ is of Ruderman-Kittel-Kasuya-Yosida (RKKY) form:[3]

$$J_{eff}^0(R) \propto R^{-3}\cos(2k_F R) . \qquad (1.1)$$

Since the interaction is mediated by the conduction electrons, when account is taken of various physical scattering processes and finite temperature, a more general form is required for $J_{eff}(R)$. It is the general form of $J_{eff}(R)$ which will determine $T_g$.

Concerted experimental efforts have been made to reveal features of $J_{eff}(R)$ by adding impurities to a spin glass and observing how the changes in $T_g$ of the resulting alloys depend on the concentrations and types of added impurities. A rich supply of experimental data has been obtained. Some important results for NM-TM spin glasses are given next. These results have not been adequately explained previously (see below).

(1) $T_g(c)$. As the concentration $c$ of magnetic impurities increases, the freezing temperature follows the empirical relation $T_g(c) \propto c^\phi$. For example, $\phi \approx 0.58$ in Au-Fe (Ref. 4) while $\phi \approx 0.69$ in Ag-Mn (Ref. 5) over the ranges studied.

(2) $T_g(c_i)$. With $c$ held fixed, $T_g(c_i)$ typically exhibits a rapid initial decrease as the concentration $c_i$ of nonmagnetic impurities increases. At higher values of $c_i$, $T_g(c_i)$ decreases more and more slowly.[6] $T_g(c_i)$ appears to flatten out and almost saturate.

(3) $T_g^{sat}(c)$. The dependence on $c$ of $T_g$ at its "saturation" value also exhibits an empirical relation of the form $T_g^{sat}(c) \propto c^\phi$ with $\phi$ slightly less than unity and different from that in (1) above. For example, $\phi = 0.91 \pm 0.03$ has been reported for Ag-Mn.[6]

(4) $T_g(c_1; c_2)$. In spin glasses having two distinct magnetic species (e.g., Mn and Fe) with concentrations $c_1$ and $c_2$, two types of behavior can occur. If $c_1$ is held fixed and $c_2$ increased from zero, $T_g(c_1, c_2)$ could increase monotonically with $c_2$ or show an initial decrease to a minimum value followed by an increase until $T_g$ exceeds its value for $c_2 = 0$.

(5) $T_g(c_{s.o.})$. At fixed concentration of a magnetic species in a NM-TM spin glass [e.g., Ag-Mn (5.5 at. %)], $T_g$ initially increases sharply as impurities with strong spin-orbit scattering (e.g., Au) are added. As the concentration, $c_{s.o.}$, of the added impurities increases, $T_g(c_{s.o.})$ increases more slowly and may tend to flatten out at a plateau value.

We next describe the theoretical picture. Consider first the variation $T_g(c_i)$ described in (2) above. There have been many theoretical works which have addressed this question by using $[J_{eff}(R)]_{av}$, the average of $J_{eff}(R)$ over all possible configurations of impurities. Because of the approximate form

$$[J_{eff}(R)]_{av} \approx J_{eff}^0(R) e^{-R/\lambda_i} , \qquad (1.2)$$

where $\lambda_i$ is the electron mean free path due to elastic scattering by nonmagnetic impurities, these works have enjoyed some degree of agreement with experiment. The approach of using $[J_{eff}(R)]_{av}$ is, however, *fundamentally wrong*, as has been shown by several investigators.[7-11] The distribution over impurity configurations of $J_{eff}(R_{ij}) \equiv J_{ij}$ is so broad that $[J_{ij}]_{av}$ is a completely inadequate representation of the effective interaction in a

given particular configuration. Instead, $([J_{ij}^2]_{\text{av}})^{1/2}$ provides a much improved estimate of the effective interaction. Indeed, while $[J_{ij}]_{\text{av}}$ exhibits strong dependence on $\lambda_i$, calculations at zero temperature of $[J_{ij}^2]_{\text{av}}$ show no dependence at all on $\lambda_i$. Thus, all accounts of $T_g(c_i)$ based on $[J_{ij}]_{\text{av}}$ or closely related modifications must be regarded as invalid. Although the investigations based on $[J_{ij}^2]_{\text{av}}$ have a more sound theoretical basis in that they take account of the broad statistical distribution of $J_{ij}$, the results presented thus far do not provide explanations for the five experimental features described above.

In this paper, we present a theory of $T_g$. Our approach accounts for experimental data on $T_g(c)$, $T_g(c_i)$, $T_g^{\text{sat}}(c)$, $T_g(c_1,c_2)$, and $T_g(c_{\text{s.o.}})$. The theory has a firm theoretical foundation and also gives a very clear picture of the physical processes involved in the behavior of $T_g$. The essential features of the theory are as follows: (i) Our calculations are based on $[J_{ij}^2]_{\text{av}}$. (ii) We include the *intrinsic sd* exchange scattering from TM ions. A consistent treatment of *sd* scattering introduces new *length scales* in the effective spin-spin interaction. Unlike $\lambda_i$, these new length scales *survive configuration averaging* to appear explicitly in $[J_{ij}^2]_{\text{av}}$. These length scales play a crucial role in accounting for the experimental trends. (iii) We work at finite temperature and explicitly retain the finite $T$ dependence in our final expressions. This leads to a finite range for the effective interaction and plays an essential role. (iv) We develop an approach to calculating the variations in $T_g$ due to changes in impurity concentrations. We express $T_g$ *directly* as a pairwise sum over interaction strengths.

The outline of the remainder of this paper is as follows. In Sec. II, we give an overview of the basic physical features of our picture of $T_g$ and describe its consequences. The essential features of our previous work[12] on effective spin-spin interactions in disordered electron systems are recalled in Sec. III and the different physical length scales are discussed. Our result for $T_g$ in terms of a sum over pairwise interaction strengths is derived in Sec. IV with a mean-field theory. The evaluation of $T_g$ as a function of nonmagnetic impurity concentration, $c_i$, and the magnetic ion concentration, $c$, is given in Secs. V and VI, respectively. $T_g$ as a function of concentration of two magnetic species is given in Sec. VII. Section VIII consists of a discussion of the effects on $T_g$ of adding impurities with strong spin-orbit interactions. A summary is given in Sec. IX.

## II. PHYSICAL DESCRIPTION OF THE THEORY

In this section we describe the basic physical picture which emerges from our theory. Our intention here is to emphasize the essential ideas, so a number of details and more complete descriptions are left to later sections.

In our approach, *sd* scattering introduces new length scales which are of the same order and are denoted collectively by $\Lambda_{sd}$. Finite temperature imposes a strictly finite range $\Lambda_T$ on the spin-spin interaction. These length scales are such that $\lambda < \Lambda_{sd} < \Lambda_T$.

The spin-spin coupling strength, denoted by $K(R)$ has the approximate form at large $R$

$$K(R) = h(R)K_0(R) , \qquad (2.1)$$

where $K_0(R) \propto R^{-3}$ is the form appropriate for two spins in an otherwise pure metal at $T = 0^+$, and

$$h(R) = \begin{cases} 1 & \text{for } R < \Lambda_{sd} \\ \gamma & \text{for } \Lambda_{sd} < R < \Lambda_T \\ 0 & \text{for } R > \Lambda_T , \end{cases} \qquad (2.2)$$

with $0 < \gamma < 1$. Note that the usual mean free path, $\lambda$, does *not* appear. Using Eqs. (2.1) and (2.2), we may describe the pairwise couplings as follows. All spin pairs having $R < \Lambda_{sd}$ are coupled with strength $K_0(R)$, all pairs with $R > \Lambda_T$ are completely uncoupled, and all pairs with $\Lambda_{sd} < R < \Lambda_T$ have coupling strength $\gamma K_0(R)$: i.e., there is a drop in coupling strength at $R = \Lambda_{sd}$. Alternatively, on the average, we may picture a fraction $\gamma$ of pairs in this range as having coupling strength $K_0(R)$, the remaining pairs as being uncoupled.

Consider the case of a fixed concentration $c$ of spins and ask what happens to $T_g$ as $c_i$ increases. We find (Sec. III) that the length scales $\Lambda_{sd}$ and $\Lambda_T$ decrease as $c_i$ increases. Decreasing $\Lambda_T$ clearly implies decoupling spin pairs. Specifically, the decrease from $\Lambda_T$ to $\Lambda_T - |\delta\Lambda_T|$, where $\delta\Lambda_T < 0$, implies the decoupling of all pairs with separation $R$ in the range $\Lambda_T - |\delta\Lambda_T| < R < \Lambda_T$. Similarly, a fraction $(1 - \gamma)$ of pairs having $R$ in the range $\Lambda_{sd} - |\delta\Lambda_{sd}| < R < \Lambda_{sd}$ also become decoupled. The decoupling of spin pairs with increasing $c_i$ implies a reduction in the overall ordering energy scale and a drop in $T_g$. A simple way to express this is

$$\delta T_g = T_g^0[(1-\gamma)\delta\Lambda_{sd}/\Lambda_{sd} + \gamma\delta\Lambda_T/\Lambda_T] , \qquad (2.3)$$

with $T_g^0$ being a constant of proportionality. [Equation (2.3) is easily derived by counting the number of spins in shells of radii $\Lambda_{sd}$ and $\Lambda_T$, with respective thicknesses $|\delta\Lambda_{sd}|$, $|\delta\Lambda_T|$ (see Sec. V).]

Alternatively, Eq. (2.3) can be integrated to give

$$T_g - T_g^* = T_g^0 \ln[(\Lambda_{sd}/\Lambda_{sd}^*)^{1-\gamma}(\Lambda_T/\Lambda_T^*)^\gamma] , \qquad (2.4)$$

where $T_g^*$ is a constant of integration having the meaning of the spin-glass transition temperature at an arbitrary reference point $\Lambda_{sd} = \Lambda_{sd}^*$, $\Lambda_T = \Lambda_T^*$.

The functional form $T_g(c_i)$ then depends on $\Lambda_{sd}(c_i)$ and $\Lambda_T(c_i)$. The *sd*-generated length scale $\Lambda_{sd}$ plays a crucial role in establishing the behavior of $T_g(c_i)$. Consider Fig. 1, which shows experimental data for $T_g$ as a function of the total resistivity $\rho$, as well as our theoretical result (solid curve) obtained from Eq. (2.4) and described in Sec. V. The crossover from rapidly decreasing $T_g$ at low $\rho$ to a slowly decreasing $T_g$ at high $\rho$ is due to a crossover in the form of $\Lambda_{sd}$, from $\Lambda_{sd} \propto \rho^{-1}$ at low $\rho$ to $\Lambda_{sd} \propto \rho^{-1/2}$ at high $\rho$. In contrast, $\Lambda_T \propto \rho^{-1/2}$ at all $\rho$. The crossover in $\Lambda_{sd}$ means that spin pairs are eliminated much more rapidly with increasing $\rho$ at low $\rho$ then they are at high $\rho$.

A similar description applies for the dependence of $T_g$
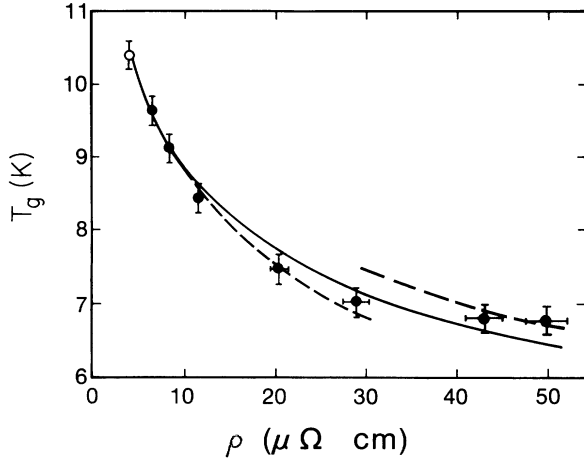
FIG. 1. The spin-glass freezing temperature $T_g$ vs the total electrical resistivity $\rho$ for Ag-Mn (2.6 at. %) with added Sb. The experimental data are from Ref. 6. The open circle indicates no added Sb. The dashed curves are low-$\rho$ and high-$\rho$ asymptotic forms, extrapolated into the intermediate-$\rho$ regime. The solid curve models the crossover as described in the text.

on $c$ in the case $c_i = 0$. Figure 2 shows experimental data and our theoretical result for Ag-Mn. The $T_g(c)$ behavior has the characteristic feature that the slope $\partial T_g(c)/\partial c$ decreases as $c$ increases. This is readily interpreted using the length scales $\Lambda_{sd}$ and $\Lambda_T$. As $c$ increases, spin pairs are added and $T_g$ increases. However, not all of the added spin pairs contribute to $T_g$. An increase in $c$ means more $sd$ scattering, decreased $\Lambda_{sd}$ and $\Lambda_T$, and the decoupling of all spin pairs in the range $\Lambda_T - |\delta\Lambda_T| < R < \Lambda_T$ and a fraction $(1-\gamma)$ in the range $\Lambda_{sd} - |\delta\Lambda_{sd}| < R < \Lambda_{sd}$. As a consequence, $T_g$ does not increase as much as it would have in the absence of "self-damping" induced by $sd$ scattering.

## C (at.% Mn)
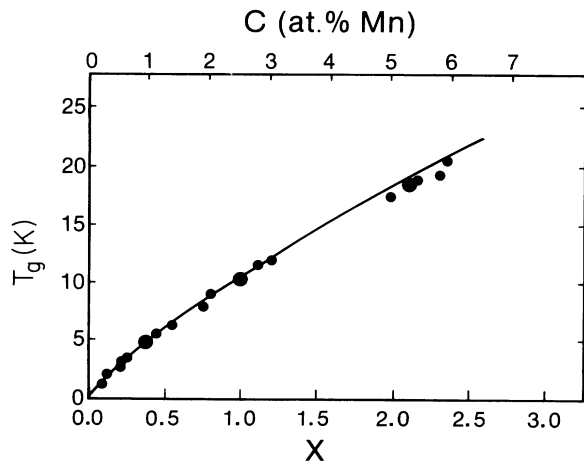


FIG. 2. $T_g$ vs concentration $c$ of Mn in Ag-Mn. The data were presented by Vier and Schultz in Ref. 6. The large dots are their results; the small dots were obtained from the literature. The curve is our theoretical result, shown as a function of $x = c/c_0$, $c_0 = 2.6$ at. %.

## III. EFFECTIVE INTERACTIONS AND LENGTH SCALES

In a previous paper, we calculated the magnitude and range of the effective spin-spin interaction in a disordered metal at finite $T$ (Ref. 12). We ensured that the intrinsic effects of $sd$ scattering and finite temperature were properly taken into account. We expressed our results in terms of the quantity $K(R)$, defined as the magnitude of the effective interaction between an average, or typical, pair of spins with separation $R = |\mathbf{R}_{ij}|$ in a typical, particular configuration, viz, $K(R)$ is obtained by averaging $|J_{\text{eff}}(\mathbf{R}_{ij})|$ over all spin pairs $(i,j)$ having $|\mathbf{R}_{ij}| = R$. For the general case where both magnetic and nonmagnetic ions are present in the metal host, we obtained

$$K(R) = j_{sd}^2 g(R) h(R) , \tag{3.1}$$

where $j_{sd}$ is the $sd$ exchange constant which enters the portion of the Hamiltonian that describes the $sd$ scattering of electrons from the TM ions, $g(R) = 2mk_F/(2\pi R)^3$, and where $h(R)$ has the following features. For $R \gtrsim \lambda$, $h(R) \sim 1$, which gives $K(R)$ the same form as in the pure metal case. Here, $\lambda$ is the total electron mean free path and includes both elastic scattering by the nonmagnetic impurities as well as $sd$ scattering by the magnetic impurities. For $R \gtrsim \Lambda_T \gg \lambda$, $h(R)$ is exponentially small [viz., $h(R) \propto e^{-R/\Lambda_T}$]: $\Lambda_T$ is the finite range of the spin-spin interaction and is given by

$$\Lambda_T = (\lambda \lambda_T/3)^{1/2} , \tag{3.2}$$

where

$$\lambda_T = T_F/(\pi k_F T) . \tag{3.3}$$

The various length scales involved in determining $T_g$, including $\Lambda_T$ and $\lambda_T$, will be discussed in the next section. For $\lambda \lesssim R \lesssim \Lambda_T$,

$$h(R) \sim [I_0(R) + I_1(R) + I_2(R) + I_3(R)]^{1/2} ,$$

$$\lambda \lesssim R \lesssim \Lambda_T , \tag{3.4}$$

where the $I_n(R)$ ($n = 0, 1, 2, 3$) depend sensitively on the ratio $c_i/c = \rho_i/\rho_{sd}$ and are, in general, quite complicated ($\rho_i$ and $\rho_{sd}$ are, respectively, contributions to the total resistivity $\rho$ due to scattering of electrons by nonmagnetic and magnetic impurities). Simple asymptotic forms exist, however, both in the regime we call "low $\rho$," in which $\rho = \rho_i + \rho_{sd}$ is, at most, a few times $\rho_{sd}$, and the regime we call "high $\rho$" where $\rho \gg \rho_{sd}$. For all $\rho$, $I_0(R) \sim \frac{3}{16}$. In the "low-$\rho$" regime, each of the other $I_n(R) \propto e^{-2R/\lambda}$ for $\lambda \lesssim R \lesssim \Lambda_T$. In the "high-$\rho$" regime they acquire the asymptotic form

$$I_n(R) \sim \frac{3}{16} \left[ 1 + \frac{2R}{\Lambda_n} + \frac{4R^2}{\Lambda_n^2} \right] e^{-2R/\lambda_n} ,$$

$$\lambda \lesssim R \lesssim \Lambda_T , \text{ high } \rho , \tag{3.5}$$

where

$$\Lambda_n \sim \lambda[(\rho/\rho_{sd} - 2n/3)/2n]^{1/2} , \text{ high } \rho . \tag{3.6}$$

The results for $h(R)$ have been presented above as

asymptotic forms. Strictly, this means that $h(r)$ asymptotically approaches unity for $R \ll \lambda$, asymptotically acquires the form of Eq. (3.4) for $\lambda \ll R \ll \Lambda_T$, asymptotically goes to zero for $R \gg \Lambda_T$, and goes smoothly between these asymptotic forms when $R = O(\lambda)$ or

$R = O(\Lambda_T)$. We do not have precise information on the form of $h(R)$ for $R = O(\lambda)$ or $R = O(\Lambda_T)$. We expect these asymptotic forms to be good approximations except when $R$ is quite close to $\lambda$ or to $\Lambda_T$, and we will therefore take

$$
h(R) = \begin{cases}
1, & \lambda_c < R < \lambda & \text{(3.7a)} \\
[I_0(R) + I_1(R) + I_2(R) + I_3(R)]^{1/2}, & \lambda < R < \Lambda_T & \text{(3.7b)} \\
0, & R > \Lambda_T, & \text{(3.7c)}
\end{cases}
$$

where the length scale $\lambda_c$ is discussed below. We will show in Sec. V that the smooth behavior of $h(R)$ for $R$ close to $\lambda$ or to $\Lambda_T$ can be readily incorporated into our theory of $T_g$.

A variety of physical length scales appear in this spin-glass problem. These length scales, $\lambda_i$, $\lambda_{sd}$, $\lambda$, $\lambda_c$, $\lambda_T$, $\Lambda_T$, and $\Lambda_n$, will be briefly discussed next.

The length scale $\lambda_i$ is the electron mean free path due to collisions with the nonmagnetic impurities, while $\lambda_{sd}$ is the mean free path due to $sd$ scattering by the magnetic species: $\lambda_i / \lambda_{sd} = \rho_{sd} / \rho_i$. The total mean free path $\lambda = 1/(1/\lambda_i + 1/\lambda_{sd})$.

The parameter $\lambda_c$ represents the *effective* lower limit spin-spin separation and must be of order of the nearest-neighbor spin-spin separation, $\lambda_{NN}$. We have introduced $\lambda_c$ in order to parametrize numerous physical features implicit in the problem of calculating $T_g$, including preasymptotic corrections[13] and statistical fluctuations in the nearest-neighbor separation.

The length scale $\lambda_T$ is the finite range at temperature $T$ for the RKKY spin-spin interaction in the case of just *two* spins in an otherwise pure metal: for $R > \lambda_T$, the interaction is exponentially small, being proportional to $e^{-R/\lambda_T}$. As Eq. (3.3) shows, $\lambda_T$ is very large. In the disordered case, however, the finite range of the effective spin-spin interaction is $\Lambda_T$. From Eq. (3.2), we see that $\Lambda_T \ll \lambda_T$ and is certainly finite at finite $T$. We will show in Secs. V–VII that the finite range $\Lambda_T$ plays a major role in determining the spin-glass transition temperature $T_g$.

The three length scales $\Lambda_n$ ($n = 1, 2, 3$) enter because of the $sd$ scattering. These length scales have an interesting $\rho$ dependence. At "low $\rho$" (where $\rho$ is, at most, a few times $\rho_{sd}$), the $\Lambda_n \sim \lambda$ to leading order, whereas at "high $\rho$" (where $\rho$ is at least several times $\rho_{sd}$) the $\Lambda_n$ are given by Eq. (3.6) to leading order. If $\rho / \rho_{sd}$ is *very* large, then Eq. (3.6) will simplify to $\Lambda_n \sim \lambda [(\rho / \rho_{sd})/2n]^{1/2}$. Thus, there is a crossover from $\Lambda_n \propto \rho^{-1}$ at low $\rho$ to $\Lambda_n \propto \rho^{-1/2}$ at *very* high $\rho$, whereas $\Lambda_T \propto \rho^{-1/2}$ at all $\rho$. This implies that, at low $\rho$, the $\Lambda_n$ decrease much more quickly with $\rho$ than $\Lambda_T$ does. This feature of the length scales will have important consequences for the overall behavior of $T_g(\rho)$, as we will see in Sec. V. Finally, we will always have $\lambda < \Lambda_n < \Lambda_T$ in the experimental situations we will consider.

## IV. A MEAN-FIELD THEORY FOR $T_g$

In this section, we derive a result for $T_g$, specializing to the case of fixed concentration $c$ of TM ions with variable concentration $c_i$ of nonmagnetic impurities, and working within mean-field theory. The experimentally determined freezing temperature typically decreases as $c_i$ increases. The basic physical idea underlying our approach is that the observed variations in $T_g$ are due to variations in the magnitude and range of the effective spin-spin interaction. We illustrate this idea by treating an Ising model spin glass within mean-field theory. Generalizing to the Heisenberg case is straightforward.

Consider an Ising model spin glass with the spins and nonmagnetic impurities arranged in a particular configuration. For $T$ just below $T_g$, mean-field theory gives

$$
\langle S_i \rangle = \frac{2S^2}{3k_B T} \sum_j J_{ij} \langle S_j \rangle \tag{4.1}
$$

for the thermal average of $S_i$, where the $J_{ij}$ are the couplings between spin pairs $(i,j)$ for the particular configuration under consideration. We may equally well write

$$
M^2(T) = \frac{1}{N} \sum_i \langle S_i \rangle^2 = \frac{2S^2}{3k_B T} \frac{1}{N} \sum_{i,j} J_{ij} \langle S_i \rangle \langle S_j \rangle. \tag{4.2}
$$

For a particular configuration, the double sum in Eq. (4.2) is a very complicated quantity. For example, as we sample various pairs $(i,j)$ of spins, the $J_{ij}$ oscillate in sign, and the $\langle S_i \rangle$ and $\langle S_j \rangle$ vary in direction (or sign). However, such variations are not completely random; if they were, the double sum would be identically zero, but it is manifestly positive. This characteristic positivity is an essential feature of the double sum which must be recognized if a suitable approximation for $T_g$ is to be obtained. A second feature of the double sum which must also be adequately recognized is the distinctive spatial variation in the $J_{ij}$ which was the subject of our previous paper, Ref. 12. We briefly review the spatial properties of $J_{ij}$, then discuss the positive character of the double sum and thereby obtain our formula for $T_g$.

There are two crucial properties of $J_{ij}$ which were reported in Ref. 12. One is that the magnitude of $J_{ij}$ is ex-

ponentially small for virtually all pairs $(i,j)$ with $R_{ij} \gtrsim \Lambda_T$, *in any typical, particular configuration*. The other is that, in addition to the regular $1/R^3$ falloff in the magnitude of $J_{ij}$—which occurs both in the pure metal and the disordered metal—there is a further decrease in the magnitude of $J_{ij}$ in the disordered case, which takes the following form: $K(R)=j_{sd}^2 g(R)$ if $R < \lambda$, whereas $K(R)=h(R)j_{sd}^2 g(R)$ if $R > \lambda$, where the reduction is by a factor $h(R) < 1$. It is essential to realize that this reduction in $K(R)$ at $R = \lambda$ results *because* the same reduction occurs for the individual $J_{ij}$; recall that $K(R)$ was obtained by averaging $J_{ij}$ over all pairs $(i,j)$ with $|\mathbf{R}_{ij}| = R$. The important consequence of these two spatial characteristics is that the double sum will decrease if nonmagnetic impurities are added to the spin glass. This decrease may be understood as follows. Adding nonmagnetic impurities will increase $\rho$ and decrease both $\Lambda_T$ and $\lambda$. Decreasing the finite range of interaction means eliminating spin pairs from the double sum in Eq. (4.2), which means a decrease in the double sum. Similarly, decreasing $\lambda$ means reducing the magnitude of $J_{ij}$ for all pairs $(i,j)$ whose separation $R_{ij}$ is such that $\lambda$ goes from greater than $R_{ij}$ to less than $R_{ij}$, which causes a further drop in the net value of the double sum. As the double sum decreases, so must $T_g$.

The behavior described in the above paragraph is retained in the formula which we will next derive for $T_g$. The derivation begins by recognizing that the manifestly positive character of the double sum arises in consequence of the off-site $(i \neq j)$ spin correlations in the spin-glass state. The relative orientation of the spins at sites $i$ and $j$—and hence the sign of $J_{ij}\langle S_i \rangle \langle S_j \rangle$—depends on the *full* distribution $\{J_{ij}\}$, but the positive character of the double sum implies an overall *tendency*— subject to frustration—for a given spin pair to take up the relative orientation favored by the sign of the specific pair's $J_{ij}$. To within a constant factor which reflects the frustration inherent in the spin glass, the double sum can then be estimated by $\sum_{i,j}|J_{ij}|M^2(T)$, which gives

$$T_g \propto k_B^{-1} N^{-1} \sum_{i,j} |J_{ij}| \ . \tag{4.3}$$

An expression for $T_g$ similar in form to Eq. (4.3) has previously been suggested by Kinzel and Fischer[14] in the low concentration limit of an Ising spin glass with sufficiently short-range interaction. The interpretation of their formulation and its predictions differ, however, from ours.

It is essential to realize that Eq. (4.3) gives $T_g$ *for a particular configuration*. As a consequence, it is important that we estimate $|J_{ij}|$ by a quantity which captures the essential characteristics innate to a particular configuration; $K(R)$ is precisely such a quantity. Since $T_g$ will vary only slightly from one configuration to another, we have

$$T_g \propto k_B^{-1} c \int d^3R \, K(R) \ , \tag{4.4}$$

where $K(R)$ is given by Eq. (3.1). This form for $T_g$ captures the essential physics which is present in a particular

configuration. To complete the specification of our formula, we introduce an overall scale factor $T_g^0$ and use Eqs. (3.1) and (3.7) to obtain

$$T_g = T_g^0 \left[ \int_{\lambda_c}^{\lambda} dR / R + \int_{\lambda}^{\Lambda_T} h(R) dR / R \right] \ , \tag{4.5}$$

where $h(R)$ is given by Eq. (3.7b), and we have specialized to the Heisenberg case. We regard Eq. (4.5) as a semiphenomenological form, with parameters $\lambda_c$ and $T_g^0$. We will comment further on these parameters in the next two sections where we calculate $T_g(c_i)$ and $T_g(c)$.

Before making use of Eq. (4.5), recall the commonly quoted form for $T_g$ which is based on assuming a Gaussian distribution for $J_{ij}$. One way to obtain this expression was given by Sherrington[15] who iterated Eq. (4.1) to obtain

$$\langle S_i \rangle = \left[ \frac{2S^2}{3k_B T} \right]^2 \sum_j' J_{ij} \sum_k' J_{jk} \langle S_k \rangle \ , \tag{4.6}$$

where the primes on the sums denote $j \neq i$ and $k \neq j$, respectively. Neglecting the correlations between the various interactions and $\langle S_k \rangle$ and using a Gaussian probability distribution to average over the distribution of interactions effectively picks out only the $k = i$ term in the $k$ sum and yields

$$T_g = \frac{2S^2}{3k_B} \left[ \sum_j' [J_{ij}^2]_{av} \right]^{1/2} \tag{4.7}$$

for the spin-glass transition temperature. The approximations leading to Eq. (4.7) are very severe. In particular, the neglect of correlations between the interactions and the spin directions is not justified for a spin glass. Indeed, it is precisely these correlations which we have taken into account in arriving at Eq. (4.3). The predictions of these two forms for $T_g$ are very different also. As discussed below, Eq. (4.7) cannot account for the experimental results in contrast to Eq. (4.3), which appears to have captured the essential physics.

## V. DEPENDENCE OF $T_g$ ON $c_i$

In this section, we calculate the spin-glass freezing temperature as a function of the concentration $c_i$ of nonmagnetic impurities for a fixed concentration $c$ of magnetic ions. In order to compare our result to experimental data, we express $T_g$ as a function of the overall resistivity $\rho$.

Extensive experimental investigation of the freezing temperature in metallic spin glasses has been carried out by Vier and Schultz[6] (VS), among others. Our attention will be primarily directed at the VS results, as these results offer a thorough test of our theoretical ideas. In particular, we will focus in this section on the VS $T_g(\rho)$ data for Ag-Mn with Sb impurities. These data span a wide range of $\rho$, from $\rho = \rho_{sd} \approx 4\mu\Omega$ cm with no Sb impurities to $\rho \approx 50\mu\Omega$ cm at the highest concentration of Sb (the Mn concentration was 2.6 at. %). The data, therefore, cover the low-$\rho$, intermediate-$\rho$ and high-$\rho$ regimes.

We require a formula for $T_g(\rho)$ which covers the whole

range of $\rho$ investigated experimentally. Our strategy is to use the low-$\rho$ and high-$\rho$ asymptotic forms for $K(R)$ (Sec. III) to obtain asymptotic forms for $T_g(\rho)$ in the low-$\rho$ and high-$\rho$ regimes, then use these results to interpolate into the intermediate-$\rho$ regime. It is not feasible to calcu-

late directly a single expression for $T_g(\rho)$ valid at all $\rho$ (Ref. 12).

Combining Eqs. (4.5), (3.7b), (3.5), and (3.6) gives the following asymptotic expression of $T_g(\rho)$ in the high-$\rho$ regime:

$$T_g(\rho) \sim T_g^0 \left[ \ln\left[ \frac{A}{\lambda_c \rho} \right] + \frac{3^{1/2}}{4} \int_1^{x_{\max}(\rho)} \left[ 1 + \sum_{n=1}^{3} f_n(x;\rho) \right]^{1/2} \frac{dx}{x} \right], \quad \text{high } \rho , \tag{5.1}$$

where $A = \rho\lambda$ is a constant whose value depends on the material,

$$x_{\max}(\rho) = \frac{\Lambda_{T_g}}{\lambda} = \left[ \frac{T_F \rho}{3\pi k_F A T_g(\rho)} \right]^{1/2} , \tag{5.2}$$

$$f_n(x;\rho) = \{1 + a_n(\rho)x + \tfrac{1}{3}[a_n(\rho)x]^2\} e^{-a_n(\rho)x} , \tag{5.3}$$

$$a_n(\rho) = 2 \left[ \frac{2n}{\rho/\rho_{sd} - 2n/3} \right]^{1/2} , \tag{5.4}$$

and the variable of integration $x \equiv R/\lambda$. Given values for the two parameters $T_g^0$ and $\lambda_c$, Eq. (5.1) is readily solved numerically for $T_g(\rho)$ in the high-$\rho$ regime. In the low-$\rho$ regime, recall that $I_n(R) \propto e^{-2R/\lambda}$ ($n = 1,2,3$), while $I_0(R) \sim \frac{3}{16}$, for $\lambda < R < \Lambda_T$. The $I_n(R)$ are therefore negligible compared to $I_0(R)$, except when $R \simeq \lambda$. As such, in order to compensate for the neglect of $I_n(R)$ for $R$ very close to $\lambda$, we introduce a parameter $\kappa$ as a multiplicative factor of the second integral in Eq. (4.5) and obtain the following asymptotic for $T_g(\rho)$ at low $\rho$:

$$T_g(\rho) \sim T_g^0 \left[ \ln\left[ \frac{\lambda}{\lambda_c} \right] + \frac{3^{1/2}}{4} \kappa \ln\left[ \frac{\Lambda_{T_g}}{\lambda} \right] \right], \quad \text{low } \rho , \tag{5.5}$$

or

$$T_g(\rho) = T_g(\rho_{sd}) \left[ 1 - C_\kappa \left[ \frac{8}{3^{1/2}} - \kappa \right] \ln\left[ \frac{\rho}{\rho_{sd}} \right] \right.$$
$$\left. - \kappa C_\kappa \ln\left[ \frac{T_g(\rho)}{T_g(\rho_{sd})} \right] \right] , \quad \text{low } \rho , \tag{5.6}$$

where $T_g(\rho)$ is the value of $T_g$ when $\rho = \rho_{sd}$ (no magnetic impurities),

$$C_\kappa = \left[ \frac{8}{3^{1/2}} \ln\left[ \frac{A}{\lambda_c \rho_{sd}} \right] + \kappa \ln\left[ \frac{T_F \rho_{sd}}{3\pi k_F T_g(\rho_{sd}) A} \right] \right]^{-1} \tag{5.7}$$

and

$$T_g^0 = \frac{8}{3^{1/2}} C_\kappa T_g(\rho_{sd}) . \tag{5.8}$$

A comparison of Eqs. (5.1) and (5.5) shows the significance of the parameter $\kappa$. One can readily verify from Eq. (5.3) that $0 < f_n(x,\rho) < 1$ for $1 < x < x_{\max}(\rho)$. If

we express the value of the second term in Eq. (5.1) as $(3^{1/2}/4)\kappa'\ln(\Lambda_{T_g}/\lambda)$, we then see that $1 < \kappa' < 2$. Recall that the factor $h(R)$ has been interpreted (Sec. IV) as the reduction in the coupling strength between moment pairs having $R > \lambda$. The high-$\rho$ coefficient $(3^{1/2}/4)\kappa'$ represents replacing the gradual reduction in coupling strength [see Eq. (5.1)] by a sudden sharp reduction at $R = \lambda$. Similarily, the low-$\rho$ factor $(3^{1/2}/4)\kappa$ in Eq. (5.5) replaces the gradual reduction by an equivalent sharp reduction taken to occur at $R = \lambda$. Had we treated the $I_n(R)$ ($n = 1,2,3$) at low $\rho$ as though they were identically zero for $\lambda < R < \Lambda_T$, we would have had $\kappa = 1$ in Eq. (5.5). This would have been too severe an approximation, as comparison with Eq. (5.1) has shown.

Our objective now is to use Eqs. (5.1) and (5.6) to fit the VS data at the high-$\rho$ and low-$\rho$ ends. Specifically, we ask if reasonable values exist for the three parameters $\kappa$, $\lambda_c$, and $T_g^0$ which provide a fit to the data. Reasonable values require $1 < \kappa < 2$, $\lambda_c$ of order $\lambda_{NN}$, and $T_g^0$ of order 1K. The dashed lines in Fig. 1 show the fits obtained for the values $\kappa = 1.4$, $\lambda_c = 7.8$ Å, $T_g^0 = 2.9$ K ($\lambda_{NN} \approx 12$ Å in 2.6 at. % Ag-Mn). We fit the theoretical, asymptotic forms to the VS experimental data by first choosing a value for $\kappa$ and using Eq. (5.6) to fit to one of the VS $[\rho, T_g(\rho)]$ data points in the low-$\rho$ regime. Note that Eq. (5.6) automatically passes through the point $[\rho_{sd}, T_g(\rho_{sd})]$. A value for $\lambda_c$ is obtained from Eq. (5.7) and a value for $T_g^0$ from Eq. (5.8). Equation (5.1) was solved numerically for the high-$\rho$ $T_g(\rho)$ curve using the $T_g^0$ and $\lambda_c$ values. We adjusted $\kappa$ until a satisfactory fit resulted at both the low-$\rho$ and high-$\rho$ ends of the VS data. In Fig. 1, we have indicated the extrapolation (dashed curves) of these low-$\rho$ and high-$\rho$ asymptotic curves into the intermediate-$\rho$ region. These extrapolations do not give a complete description of the VS data. As a result, we require a representation of the $\rho$ dependence which interpolates correctly between these two asymptotic limits. We have developed such an interpolation and the result is indicated in Fig. 1 by the solid curve which clearly provides a much improved description of the data. The basis for this interpolation is most easily described in connection with a physical interpretation of the behavior of $T_g(\rho)$ in Fig. 1. A simplified version of this interpretation was given in Sec. II.

The trends exhibited by $T_g(\rho)$ result directly from combined physical effects of $sd$ scattering, potential scattering, and finite temperature, and can be interpreted

as follows. The length scales $\Lambda_n$ and $\Lambda_T$ all decrease as nonmagnetic impurities are added to increase $\rho$. As a given length scale $\Lambda$ ($\Lambda_n$ or $\Lambda_T$) drops by $\delta\Lambda$, spins within a shell of thickness $\delta\Lambda$ and radius $R = \Lambda$ are decoupled from a spin at the center of the shell. The decoupling of spins is obvious for the finite range $\Lambda_T$, but strictly speaking, the coupling strength is simply *reduced* by a factor $(3^{1/2}/4)\kappa$ in the case of $\Lambda_n$. However, an equivalent picture is that a fraction $1-(3^{1/2}/4)\kappa$ of spins have been completely decoupled and that the coupling strength of the remaining spins has been unaltered. The simple picture of spin pairs being decoupled as $\rho$ increases implies that the overall ordering energy is reduced and $T_g$ falls.

Consider more fully the role of the $sd$-generated length scales $\Lambda_n$. The transition from a rapidly decreasing $T_g$ at the smallest values of $\rho$ to a more slowly decreasing $T_g$ at the high-$\rho$ extreme is due to a combination of two effects. First, as $\rho$ increases and spins decouple, the rate at which ordering energy is lost (and $T_g$ falls) *decreases* in magnitude. It is easily seen from the picture of decoupling spins that $\partial T_g/\partial\rho \propto -\rho^{-1}$, which leads to a gradual tendency for $T_g$ to "flatten out" as $\rho$ increases (see Fig. 1). The second effect is a crossover in the $\rho$ dependence of $\Lambda_n$ from $\Lambda_n \propto \rho^{-1}$ in the $sd$-dominated scattering regime at low $\rho$ to

$$\Lambda_n \sim \lambda[(\rho/\rho_{sd}-2n/3)/2n]^{1/2}$$

in the high-$\rho$ regime where both potential and $sd$ scattering are important. (When $\rho$ is very much larger than $\rho_{sd}$, $\Lambda_n \propto \rho^{-1/2}$, but we do not quite reach this behavior in the VS data of Fig. 1). This crossover in the $\rho$-dependence of $\Lambda_n$ contributes further to the tendency for $T_g$ to "flatten out" at high $\rho$.

It is necessary to include the crossover behavior of $\Lambda_n$ in the development of an interpolation formula for $T_g(\rho)$. In order to test the sensitivity of the interpolated $T_g(\rho)$ curve we modeled the crossover in different ways. For example, a simple way to model the crossover is to form a linear combination of the low-$\rho$ and very high-$\rho$ asymptotic forms, $\lambda$ and $(2n)^{-1/2}\lambda(\rho/\rho_{sd})^{1/2}$, respectively. Since the $\Lambda_n$ are of the same order even at high $\rho$, we take the middle value ($n = 2$) and use

$$\Lambda_{sd}(\rho) = \tfrac{2}{3}[\lambda + \tfrac{1}{2}\lambda(\rho/\rho_{sd})^{1/2}] \tag{5.9}$$

to interpolate for the $sd$ length scales $\Lambda_n$.[16] Combining Eq. (5.9) with the physical picture described above, we write

$$\delta T_g = T_g^0[(1-\gamma)\delta\Lambda_{sd}/\Lambda_{sd} + \gamma\delta\Lambda_T/\Lambda_T] \tag{5.10}$$

for the variation in $T_g$, where $\gamma = (3^{1/2}/4)\kappa$. Solving for $T_g(\rho)$ gives

$$T_g(\rho) = T_g(\rho_{sd}) - T_g^0 \left[ \left[1-\frac{\gamma}{2}\right]\ln\left[\frac{\rho}{\rho_{sd}}\right] \right.$$
$$-(1-\gamma)\ln\left[\frac{2+(\rho/\rho_{sd})^{1/2}}{3}\right]$$
$$\left. +\frac{\gamma}{2}\ln\left[\frac{T_g(\rho)}{T_g(\rho_{sd})}\right] \right] \tag{5.11}$$

as a possible interpolation formula. We return to this formula below, but first describe an alternative approach in which we model the crossover directly in terms of a $\rho$-dependent effective exponent $\theta(\rho)$, viz.,

$$\Lambda_{sd}(\rho) = \Lambda_{sd}(\rho_{sd})\left[\frac{\rho}{\rho_{sd}}\right]^{-\theta(\rho)}, \tag{5.12}$$

where $\Lambda_{sd}(\rho_{sd}) = A/\rho_{sd}$. We require $\theta(\rho) \sim 1$ as $\rho \to \rho_{sd}^+$, and $\theta(\rho) \sim \frac{1}{2}$ as $\rho/\rho_{sd} \to \infty$. There are, of course, many possible choices for $\theta(\rho)$. We tested the simple form

$$\theta(\rho) = (\rho/\rho_{sd})^{-\nu}, \tag{5.13}$$

obtaining a value for the constant $\nu$ by equating the $\Lambda_{sd}(\rho)$ of Eq. (5.12) with the high-$\rho$ form, Eq. (3.6), for $\Lambda_n$ ($n = 2$) at the highest $\rho$ value for the VS data in Fig. 1. We found $\nu \approx 0.11$, and $\theta \approx 0.8$ at this highest $\rho$ value. Combining Eqs. (5.12), (5.13), and (5.10) gives

$$T_g(\rho) = T_g(\rho_{sd}) - T_g^0 \left\{ \left[\frac{\gamma}{2} + (1-\gamma)\left[\frac{\rho}{\rho_{sd}}\right]^{-\nu}\right]\ln\left[\frac{\rho}{\rho_{sd}}\right] \right.$$
$$\left. +\frac{\gamma}{2}\ln\left[\frac{T_g(\rho)}{T_g(\rho_{sd})}\right] \right\} \tag{5.14}$$

as an alternative to Eq. (5.11) for the interpolation formula. The solid curve plotted in Fig. 1 is actually Eq. (5.14). However, the curve specified by Eq. (5.11) results in virtually the same curve for $T_g(\rho)$. Sensitivity to the precise modeling scheme is minimal provided the essential physics is included correctly.

Note that the solid curve has not quite merged onto the high-$\rho$ asymptote. This is because the extreme high-$\rho$ asymptotic form for $\Lambda_{sd}$, the second term on the right-hand side of Eq. (5.9), has not quite been reached at $\rho \approx 50\mu\Omega$ cm for Ag-Mn with 2.6 at. % Mn, as is readily verified from Eq. (3.6).

We emphasize that if $sd$ scattering had been neglected the crossover effect discussed in this section would have been missed, and a complete description of the $T_g(\rho)$ data over the entire range of $\rho$ would not have been obtained.

We have also applied our $T_g(\rho)$ theory to other materials. Some results will be given in Sec. VI.

## VI. DEPENDENCE OF $T_g$ ON $c$

Our basic formula for $T_g$ may also be applied to the case where only magnetic impurities exist within the metallic host. In this case, Eq. (4.4) leads directly to an expression very similar to Eq. (5.5):

$$T_g(c) = T_g^0 \frac{c}{c_0} \left[ \ln \left[ \frac{\lambda}{\lambda_c} \right] + \gamma \ln \left[ \frac{\Lambda_{T_g}}{\lambda} \right] \right] , \qquad (6.1)$$

where $T_g^0$ and $\gamma$ are the same constants as in Sec. V, $c$ is the concentration of magnetic ions, and $c_0$ is a "reference" concentration of magnetic ions. For example, $c_0$ is the 2.6 at. % concentration of Mn in the VS Ag-Mn data of Sec. V. Note that Eq. (6.1) is the "low-$\rho$" asymptotic form for $T_g(c)$. We use this form because the experimental data we compare our results to are always in the "low-$\rho$" regime (see below).

We express $\lambda$, $\lambda_c$, and $\Lambda_{T_g}$ explicitly as functions of $c$, which gives $\lambda = A / \rho_{sd}(c) = B/c$, $\lambda_c = B'/c^{1/3}$, and

$$\Lambda_{T_g}/\lambda = \{ T_F c / [3\pi k_F B T_g(c)] \}^{1/2} ,$$

where $A$, $B$, and $B'$ are constants. Thus, Eq. (6.1) becomes

$$t(x) = x - \alpha_1 x \ln x + \alpha_2 x \ln[x / t(x)] , \qquad (6.2)$$

where $x \equiv c/c_0$, $t(x) \equiv T_g(c)/T_g(c_0)$, and $\alpha_1 = 0.19$ and $\alpha_2 = 0.086$ are constants which are *already fixed* in terms of the parameters used to fit $T_g(\rho)$ to the VS experimental data of Fig. 1. More specifically,

$$\alpha_1 = \frac{2}{3} \left[ \ln \left[ \frac{A}{\lambda_c^0 \rho_{sd}^0} \right] + \frac{\gamma}{2} \ln \left[ \frac{T_F \rho_{sd}^0}{3\pi k_F A T_g(c_0)} \right] \right]^{-1} \qquad (6.3)$$

and

$$\alpha_2 = \tfrac{3}{4}\gamma\alpha_1 , \qquad (6.4)$$

where $\lambda_c^0 = \lambda_c(c_0)$, $\rho_{sd}^0 = \rho_{sd}(c_0)$, and $T_g(c_0) = [T_g(c)]_{c=c_0}$ (this should not be confused with $T_g^0$).

We emphasize that there are *no free parameters* in Eq. (6.2). Of course, the values given above for $\alpha_1$ and $\alpha_2$ are characteristic of Ag-Mn. Other materials, such as Cu-Mn (see below), will also have their own characteristic values of $\alpha_1$ and $\alpha_2$. Equation (6.2) may be regarded as a prediction of the theory in the sense that the VS $T_g(\rho)$ data for Ag-Mn have been used to obtain values for $\alpha_1$ and $\alpha_2$, and knowing only $T_g(c_0)$ we predict the values of $T_g(c)$ for other concentrations. In any case, Eq. (6.2) provides a test of the theory. In Fig. 2, we show $T_g(c)$ for Ag-Mn. The data points are those given in Fig. 2(b) of VS. The solid line is our theoretical result, Eq. (6.2). Note that $c \lesssim 2.5 c_0$ in Fig. 2, which means $\rho_{sd}(c) \lesssim 2.5$ $\rho_{sd}(c_0) \approx 11\mu\Omega$ cm, so that the data fall well within the low-$\rho$ regime discussed in Sec. V.

The physical interpretation of the behavior of $T_g(c)$ is as follows. If the concentration is increased by $\delta c$ from an initial value $c$, the growth in the average ordering energy per spin will tend to be proportional to $\delta c$, so that the increment $\delta T_g$ in the freezing temperature will also tend to be proportional to $\delta c$ [see Eq. (4.4)]. If this were the whole picture we would have $T_g(c) \propto c$. However, as the concentration of magnetic ions increases, the intrinsic *sd* scattering of electrons increases, and the important
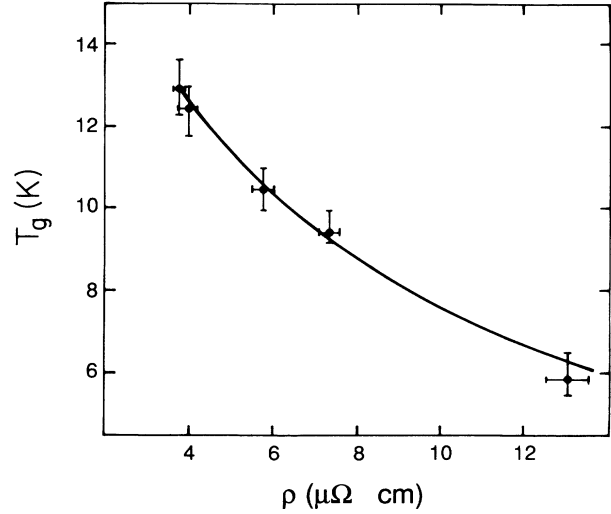


FIG. 3. $T_g$ vs $\rho$ for Cu-Mn (2.2 at. %). The experimental data are from Ref. 17. The curve is our theoretical result. Compare with Fig. 1.

length scales $\Lambda_{sd} = \lambda$ and $\Lambda_{T_g}$ decrease. The decreases in $\Lambda_{sd}$ and $\Lambda_{T_g}$ imply the elimination of some spin pairs from contributing to $T_g$, viz., some of the spin pairs that are formed when $c$ is increased do *not* contribute to $T_g$ because $\Lambda_{sd}$ and $\Lambda_{T_g}$ decrease. As a consequence, the increment $\delta T_g$ is not quite in proportion to $\delta c$, $\delta T_g/\delta c$ decreases as $c$ increases, and $T_g(c)$ has the form shown in Fig. 2.

We also point out that the curve in Fig. 2 is practically indistinguishable from the empirical power law $t(x) = x^\phi$ with $\phi = 0.81$. However, Eq. (6.2) has a clear physical basis and a solid theoretical foundation and is preferable to the empirical form in this respect. It is important to note from Eq. (6.2) that the asymptotic behavior of $T_g(c)$ at low concentration is
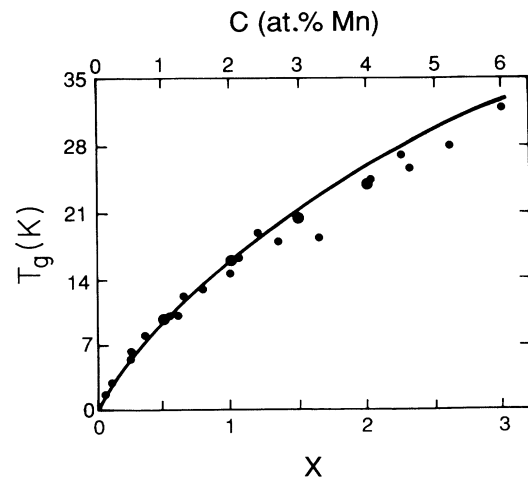


FIG. 4. $T_g$ vs $c$ for Cu-Mn. The data were presented in Ref. 6. The curve is our theoretical result with $c_0 = 2.0$ at. %. Compare with Fig. 2.

$$T_g(c) \propto -c \ln c \ , \quad c \ll 1 \ . \tag{6.5}$$

This behavior is to be contrasted with a variety of other theoretical approaches which predict that $T_g(c) \propto c$ at low concentration.

We have performed a similar analysis for other materials. In Fig. 3, we show our $T_g(\rho)$ fit to the data reported by Hitzfeld and Ziemann[17] for Cu-Mn with 2.2 at. % Mn. The parameters $\lambda_c$ and $T_g^0$ required for that fit were used to generate the parameter free curve for $T_g(c)$ for Cu-Mn, shown in comparison to experimental data in Fig. 4. The data points in Fig. 4 were given in Fig. 2(a) of VS.

Finally, we can apply precisely the same procedures to describe the $c$ dependence of $T_g^{\mathrm{sat}}(c)$, i.e., in the high-$\rho$ regime. The result for $t^{\mathrm{sat}}(x) = T_g^{\mathrm{sat}}(c)/T_g^{\mathrm{sat}}(c_0)$ has the same structure as Eq. (6.2) but the constants corresponding to $\alpha_1$ and $\alpha_2$ must be determined using the high-$\rho$ forms. For Ag-Mn, their values are 0.055 and 0.039, respectively. The concentration dependence of $T_g^{\mathrm{sat}}(c)$ is also well described by the empirical power law $t^{\mathrm{sat}}(x) = x^\phi$, where now $\phi = \phi^{\mathrm{sat}} = 0.95$. This is in excel-

lent agreement with the result $\phi^{\mathrm{sat}} = 0.91 \pm 0.03$ quoted by VS [see also their Fig. 2(b)].

## VII. TWO MAGNETIC SPECIES

We next consider the behavior of the freezing temperature in a metallic spin glass having two distinct magnetic species. We take the concentration $c_1$ of one type of magnetic ion to be fixed and calculate the freezing temperature $T_g$ as a function of the concentration $c_2$ of the second type. Experimentally, two qualitatively different types of behavior have been reported.[6] In some cases $T_g(x)$ is monotonic increasing with $x \equiv c_2/c_1$. In others $T_g(x)$ shows an initial decrease to a minimum, then increases with increasing $x$. Both types of behaviors emerge in the formulation presented below and are readily understood in terms of physical ideas described earlier in this paper.

Mean-field theory gives equations for the thermal averages $\langle S_i^{(1)} \rangle$ and $\langle S_{j'}^{(2)} \rangle$ of the spins of the two types of magnetic moments:

$$\frac{1}{N_1} \sum_i \langle S_i^{(1)} \rangle^2 = \frac{S_1(S_1+1)}{3k_B T} \frac{1}{N_1} \sum_i \sum_{a,b} \left[ \sum_{j\,(\neq i)} J_{ijab}^{(1)} \langle S_{ia}^{(1)} \rangle \langle S_{jb}^{(1)} \rangle + \sum_{j'} J_{ij'ab}^{(12)} \langle S_{ia}^{(1)} \rangle \langle S_{j'b}^{(2)} \rangle \right] \tag{7.1}$$

and

$$\frac{1}{N} \sum_{i'} \langle S_{i'}^{(2)} \rangle^2 = \frac{S_2(S_2+1)}{3k_B T} \frac{1}{N_2} \sum_{i'} \sum_{a,b} \left[ \sum_{j'\,(\neq i')} J_{i'j'ab}^{(2)} \langle S_{i'a}^{(2)} \rangle \langle S_{j'b}^{(2)} \rangle + \sum_j J_{i'jab}^{(12)} \langle S_{i'a}^{(2)} \rangle \langle S_{jb}^{(1)} \rangle \right] , \tag{7.2}$$

where $J^{(1)}$, $J^{(2)}$, and $J^{(12)}$ denote the coupling between spin pairs both of "type 1," both of "type 2," and one of each type, respectively. These equations were obtained in the same manner as Eq. (4.2).

Equations (7.1) and (7.2) are complicated, coupled equations. Nevertheless, by making some reasonable simplifications, we can proceed along the lines of Secs. V and VI to derive expressions for $T_g^{(1)}(x)$ from Eq. (7.1) and $T_g^{(2)}(x)$ from Eq. (7.2). We find that several parameters appear. As a consequence, it is, of course, possible to fit the VS data very well. This does not, however, provide any meaningful insight. Instead, we choose to emphasize the physical features which emerge. With this goal in mind, we focus on the physical ideas and omit the detailed calculations.

The principal quantities which appear in the expressions for $T_g^{(1)}(x)$ and $T_g^{(2)}(x)$ are the length sales $\lambda$, $\Lambda_{T_g}$, and three cutoff lengths, $\lambda_c^{(1)}$, $\lambda_c^{(2)}$, and $\lambda_c^{(3)}$, where $\lambda_c^{(1)}$ and $\lambda_c^{(2)}$ are the lower cutoffs defined in Sec. V, for spin types "1" and "2," respectively, while $\lambda_c^{(3)}$ is the effective, shortest distance between spins of *different* types. Using appropriate forms for the $\lambda_c^{(p)}$ (see Sec. VI), $T_g^{(1)}(x)$ and $T_g^{(2)}(x)$ are expressed in terms of the ratio of concentrations $x = c_2/c_1$. Setting $T_g^{(1)}(x) = T_g^{(2)}(x)$ completes the calculation.

Despite the involvement of several parameters, the two different qualitative behaviors of $T_g(x)$ observed experi-

mentally (and described in the opening paragraph) readily emerge from the expression we calculate. The key quantities involved are the coupling strengths $J_1 \propto [j_{sd}^{(1)}]^2$, $J_2 \propto [j_{sd}^{(2)}]^2$, and $J_{12} \propto [j_{sd}^{(12)}]^2$. The ratio $J_{12}/J_1$ (viz, the ratio of coupling strengths between pairs of opposite types, to coupling strengths between type-1 pairs) plays a major role in determining the behavior of $T_g(x)$. The qualitative behavior of $T_g(x)$ decreasing with the addition of type-2 moments requires that $J_{12}/J_1$ be considerably smaller than unity. If $J_{12}/J_1$ is of order unity or greater, the opposite trend of $T_g(x)$ increasing with $x$ results.

The physical processes underlying this behavior in $T_g$ are readily extracted from our model. As moments of type 2 are added, $T_g$ tends to increase for the same reasons given in Sec. VI, and also because the important length scales $\lambda_c^{(2)}$ and $\lambda_c^{(1,2)}$ decrease.[18] However, the addition of type-2 moments also results in $\lambda$ and $\Lambda_{T_g}$ decreasing, which eliminates moment pairs from contributing to $T_g$ so that $T_g$ tends to decrease. There is thus a competition between increased $sd$ scattering (tending to lower $T_g$) and diminished nearest-neighbor distances (tending to raise $T_g$). Provided that $J_2$ and $J_{12}$ are sufficiently smaller than $J_1$, the $sd$ scattering will initially dominate as type-2 moments are added and $T_g$ will fall. If enough moments are added, the nearest-neighbor effects will eventually win out, $T_g$ will stop decreasing

and will eventually increase beyond its original value. However, if $J_2$ is of order of or greater than $J_1$, the nearest-neighbor effects will always win out and $T_g$ will increase monotonically.

## VIII. DEPENDENCE OF $T_g$ ON $c_{s.o.}$

The behavior of $T_g$ is complex when impurities with strong spin-orbit interactions (e.g., Au,Pt) are added. There are two major competing effects. First, the added strong spin-orbit coupling enhances magnetic anisotropy fields and leads to an anisotropic spin-spin interaction of Dzyaloshinsky-Moriya form as shown by Fert and Levy.[19] The resulting anisotropy sharply increases $T_g$. In fact, Bray, Moore, and Young have argued that $T_g$ would be strictly zero in the absence of anisotropy.[20] Numerical data from Monte Carlo simulations of models for metallic spin glasses support this view although the possibility of a small but finite $T_g$ is not ruled out.[21,22] On the other hand, Ferd, de Courtenay, and Bouchiat[23] have analyzed the experimental data of Vier and Schultz[6] and have suggested that RKKY-type Heisenberg spin glasses have a nonzero $T_g$ in the limit of zero anisotropy. The data in question were taken on Cu-Mn (4.0 at. %) with added Au or Pt and on Ag-Mn (5.5 at. %) with added Cu or Au. The issue of whether $T_g$ is zero for fully isotropic interactions is not crucial for the present discussion. The most important point is that the anisotropic interactions provide a mechanism which does increase $T_g$ markedly.

Vier and Schultz[6] have shown that the total anisotropy constant, $K_{anis}$, at 2.0 K is linear in the concentration of Au, $c_{s.o.}$, for the full range of $c_{s.o.}$ up to 5% for the spin-glass alloys Cu-Mn and Ag-Mn with added Au. However, the increase in $T_g(c_{s.o.})$ with increasing $c_{s.o.}$ is not linear and $T_g$ tends to flatten out at the higher values of $c_{s.o.}$. The reduction in the rate of increase of $T_g(c_{s.o.})$ with increasing $c_{s.o.}$ is due to a second major effect. The spin-orbit interactions break time-reversal symmetry and the scattering of conduction electrons from spin-orbit impurities leads to a loss in coherence of spin-spin interactions. As a consequence, length scales $\Lambda_{s.o.}$ associated with spin-orbit appear in $[J_{ij}^2]_{av}$, as was pointed out by Stephen and Abrahams.[24] Within our formulation of $T_g$ in Sec. IV, the $\Lambda_{s.o.}$ length scales lead to suppression of $T_g$ in the same way as do the $\Lambda_{sd}$ length scales; the physical reason is the same in both cases.

The experimental trends found by Vier and Schultz[6] (see their Fig. 3) and further discussed by Fert, de Courtenay, and Bouchiat[23] show clearly the competing effects of anisotropy enhancement and "self-damping" suppression of $T_g$ due to the spin-orbit interactions. Good fits to the data can certainly be obtained, but in view of the number of additional parameters which must be specified such fits would not add further insight at this point and are omitted just as in the previous section.

## IX. SUMMARY

The distribution of effective spin-spin interactions $J_{ij}$ is broad in the metallic spin glasses of present interest.

Fluctuations of $J_{ij}$ about the configuration averaged mean value $[J_{ij}]_{av}$ are very large relative to $[J_{ij}]_{av}$. As a result, the effective interactions for a given sample in a particular configuration cannot be properly described by $[J_{ij}]_{av}$. Many attempts have been made in the past to describe a variety of experimental results by using $[J_{ij}]_{av}$ or a closely related modification. All of these attempts must be regarded as unsatisfactory, irrespective of any apparent empirical success. It has been shown that they have no fundamental foundation, and an alternative approach has emerged from the work of several investigators.[7-11] The quantity $([J_{ij}^2]_{av})^{1/2}$ has been found to be a more suitable measure of the strength of the effective interaction between two spins at $\mathbf{R}_i$ and $\mathbf{R}_j$. We follow this procedure.

To describe the dependence of the effective indirect exchange interactions on the composition of the spin glass, we find that it is necessary to take account of intrinsic $sd$ exchange scattering and to maintain finite temperature explicitly in the theory. The $sd$ exchange scattering (and any other interaction which breaks time-reversal symmetry) introduces length scales which strongly affect the strength of the interaction and its dependence on impurity concentration at a given spin-spin separation $R$. The role of finite temperature is to provide a possibly large but strictly finite range or cutoff for the effective interactions. Finally, we have constructed a theory for $T_g$ for these systems which properly takes account of the correlations which exist between the "random" interactions and the distribution of local spin orientations in the spin glass. An explicit form has been given in a mean-field approximation, $T_g \propto \sum_i ([J_{ij}^2]_{av})^{1/2}$. Although approximate, we believe this result accurately depicts the *variation* of $T_g$ with the concentration of nonmagnetic and magnetic impurities. Our physical picture also applies to the case of added impurities with strong spin-orbit interactions. In fact, we have provided a comprehensive account and physical picture of all of the features of the extensive data of Vier and Schultz.[6]

We want to point out very clearly that the experimental results cannot be explained by making use of the commonly used expression for $T_g$, namely, $T_g \propto (\sum_i [J_{ij}^2]_{av})^{1/2}$. This expression can be arrived at in a number of ways, using mean-field theories just as we have, but its predicted concentration dependence is incorrect.

Of course, it is clear that we have omitted some physical effects which may be quantitatively significant, particularly at high impurity concentration in some systems. However, the physical effects which we have described in terms of the effective interaction strength and its role in determining variations in $T_g$ are essential for all metallic spin glasses.

*Present address: Department of Physics, University of Lethbridge, Lethbridge, Alberta, Canada T1K 3M4.

[1]A. Blandin and J. Friedel, J. Phys. Rad. **20**, 160 (1959).

[2]Numerous excellent review articles and books exist, including J. A. Mydosh and G. J. Nieuwenhuys, in *Ferromagnetic Materials*, edited by E. P. Wohlfarth (North-Holland, Amsterdam, 1980), Vol. 1, p. 71; Peter J. Ford, Contemp. Phys. **23**, 141 (1982); K. Binder and A. P. Young, Rev. Mod. Phys. **58**, 801 (1986); D. Chowdhury, *Spin Glasses and Other Frustrated Systems* (Princeton University Press, Princeton, 1986); K. H. Fischer and J. A. Hertz, *Spin Glasses* (Cambridge University Press, Cambridge, 1991).

[3]The pure metal case at $T=0^+$ is described in C. Kittel, *Quantum Theory of Solids* (Wiley, New York, 1963), pp. 360–364.

[4]V. Cannella and J. A. Mydosh, Phys. Rev. B **6**, 4220 (1972).

[5]V. Cannella and J. A. Mydosh, *Magnetism and Magnetic Materials-1973 (Boston)*, Proceedings of the 19th Annual Conference on Magnetism and Magnetic Materials, AIP Conf. Proc. No. 18, edited by C. D. Graham and J. J. Rhyne (AIP, New York, 1974), p. 651; I. N. Ibrahim, E. Chock, R. Orbach, and I. Schuller, Phys. Rev. B **18**, 3559 (1978).

[6]D. C. Vier and S. Schultz, Phys. Rev. Lett. **54**, 150 (1985).

[7]P. F. de Chatel, J. Magn. Magn. Mater. **23**, 28 (1981).

[8]A. Yu. Zyuzin and B. Z. Spivak, Pis'ma Zh. Eksp. Teor. Fiz. **43**, 185 (1986) [JETP Lett. **43**, 234 (1986)].

[9]L. N. Bulaevskii and S. V. Panyukov, Pis'ma Zh. Eksp. Teor. Fiz. **43**, 190 (1986) [JETP Lett. **43**, 240 (1986)].

[10]G. Bergmann, Phys. Rev. B **36**, 2469 (1987).

[11]A. Jagannathan, E. Abrahams, and M. Stephen, Phys. Rev. B

[12]M. R. A. Shegelski and D. J. W. Geldart, Phys. Rev. B (to be published). A brief account of this work was given in M. R. A. Shegelski and D. J. W. Geldart, Solid State Commun. **79**, 769 (1991).

[13]Corrections to the large-$R$ ($R \gg k_F^{-1}$) form of the effective interactions have been studied in the pure metal limit by G. Malmström, D. J. W. Geldart, and C. Blomberg, J. Phys. F **6**, 233 (1976); **6**, 1953 (1976); see also, P. M. Levy and Q. Zhang, Phys. Rev. B **33**, 665 (1986). These preasymptotic corrections can be neglected in the regime of $k_F\lambda \gg 1$ and low concentration of TM ions. The weak corrections to the interaction strength for $R < \lambda$ found by A. Jagannathan, Phys. Rev. B **40**, 5980 (1989), can also be neglected.

[14]W. Kinzel and K. H. Fischer, J. Phys. F **7**, 2163 (1977).

[15]D. Sherrington, J. Phys. C **8**, L208 (1975).

[16]The factor $\frac{2}{3}$ in Eq. (5.9) ensures that $\Lambda_{sd}(\rho)=\lambda$ when $\rho=\rho_{sd}$.

[17]M. Hitzfeld and P. Ziemann, Phys. Rev. B **32**, 3026 (1985).

[18]This latter process also occurs in the case considered in Sec. VI.

[19]A. Fert and P. M. Levy, Phys. Rev. Lett. **44**, 1538 (1980).

[20]A. J. Bray, M. A. Moore, and A. P. Young, Phys. Rev. Lett. **56**, 2641 (1986).

[21]J. D. Reger and A. P. Young, Phys. Rev. B **37**, 5493 (1988).

[22]A. Chakrabarti and C. Dasgupta, J. Phys. C **21**, 1613 (1988).

[23]A. Fert, N. de Courtenay, and H. Bouchiat, J. Phys. (Paris) **49**, 1173 (1988).

[24]M. J. Stephen and E. Abrahams, Solid State Commun. **65**, 1423 (1988).

37, 436 (1988).